GEOLOGICA CARPATHICA, 49, 1, BRATISLAVA, FEBRUARY 1998
5–14

PRELIMINARY RESULTS FROM ROCK MAGNETIC ANALYSES OF QUATERNARY AND TERTIARY BASALTS FROM THE GULF COAST OF MEXICO

JOHN-PAUL J. POLLARD[1], GRAHAM J. SHERWOOD[1] and HARALD BÖHNEL[2]

[1]School of Biological and Earth Sciences, Liverpool John Moores University, Byrom Street, Liverpool L3 3AF, UK
[2]Instituto de Geofisica, UNAM, Cd. Universitaria, 04510 Mexico-City, Mexico

(Manuscript received March 18, 1997; accepted in revised form December 11, 1997)

Abstract: As the foundation for a paleomagnetic study of the Gulf Coast of Mexico, rock magnetic measurements were carried out on basaltic samples from 40 sites in the Gulf Coast region. Strong-field thermomagnetic and hysteresis techniques as well as room and low temperature susceptibility analyses were employed. These measurements show that the samples contain titanomagnetites with domain states from single- to multi-domain, with few superparamagnetic grains. Most samples have undergone at least partial deuteric oxidation though a significant quantity have not. The titanomagnetites have a range of compositions from Ti-poor to Ti-rich, where the latter appear to have endured varying degrees of maghematization.

Key words: Mexico, Gulf Coast, basalts, rock magnetism.

Introduction and geological setting

As part of a project to determine paleomagnetically the long-term tectonic characteristics of the Gulf Coast of Mexico, samples have been taken from various localities within the Gulf Coast region for rock magnetic investigation. This investigation is needed to give a detailed knowledge of the magnetic mineralogy and domain states of the magnetic minerals as it is essential that the rock is carrying a primary remanent magnetization for tectonic reconstruction.

The study area (see Fig. 1 and Tables 1a and 1b) includes the eastern end of the Trans-Mexican Volcanic Belt (TMVB) and a large portion of the Eastern Alkaline Province (EAP) as described by Robin (1976, 1982) and Thorpe (1977). The volcanism of the TMVB is related to subduction of the Rivera and Cocos plates along the Middle America Trench (Nixon 1982; Burbach et al. 1984; Nixon et al. 1987; Böhnel 1997). The TMVB itself is composed of Tertiary volcanic and intrusive rocks of andesitic and basaltic composition. The part of the TMVB in the study area is made up primarily of andesites and dacites with ages less than 15 Ma (Cantagrel & Robin 1979). The EAP is a discontinuous belt of associated alkaline and hyperalkaline magmatic suites that lie between the Trans-Pecos province, southern Texas, and the Tuxtla Massif, southern Veracruz. EAP volcanism extended southward during late Tertiary times. The alkaline lavas of Texas have ages between 43 and 16 Ma (Parker & McDowell 1973; Barker 1977). In Mexico alkaline magmatism began in Oligocene times in the north, in the Miocene in the central zone, and in Pliocene–Quaternary times in the south (Robin & Tournon 1978; Cantagrel & Robin 1979). The EAP suites are of Pliocene–Quaternary age within the study area, and are composed of a range of alkaline rocks including nephelinites, basanites and alkali basalts (Thorpe 1977; Robin & Tournon 1978). The cause of the EAP volcanism is uncertain but is probably associated with the occurrence of north–south rifting along the border of the coastal plain and Altiplano regions 9–3 Ma ago (Cantagrel & Robin 1979; Robin 1982).

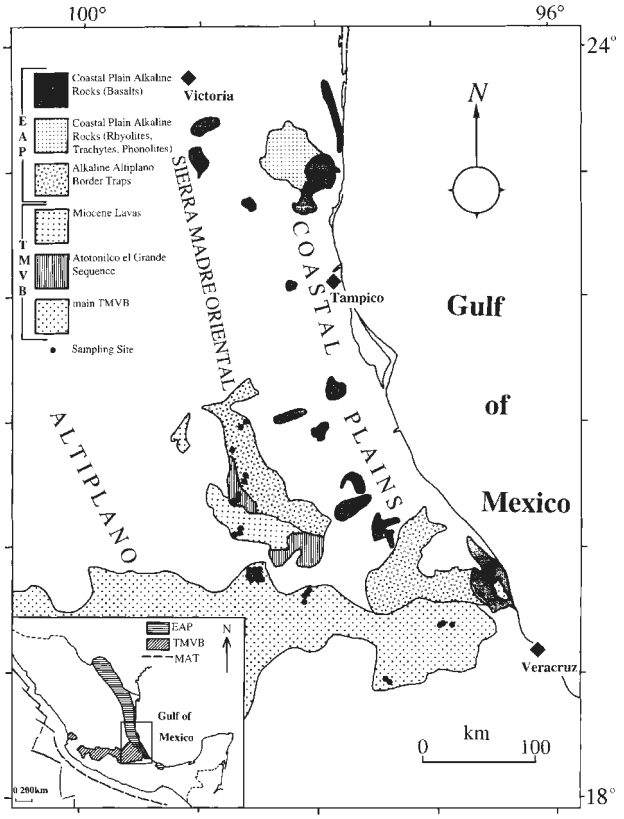

Fig. 1. Map showing the general geology of the study area and sample site locations (after Cantagrel & Robin 1979). EAP—eastern alkaline province; TMVB—trans-Mexican volcanic belt; MAT—middle america trench (inset map).

Table 1a: Site location with rock type and approximate age for EAP sites. Sites MOL A and MOL B are from the same location but are slightly different rock types.

EAP SITES		
Site	**Location**	**General rock type and approx. age.**
TEC	19°75.94N, 96°55.57W	Fine grained basalt with occasional small (< 2 mm diam.) vesicles. Quaternary.
DED	19°80.84N, 96°53.67W	Fine grained basalt containing very small (< l mm diam.) vesicles. Quaternary.
SAN	19°86.69N, 96°50.69W	Fine grained basalt with some yellow alteration. Rare vesicles. Quaternary.
POZ	20°47.35N, 97°63.84W	Very fine grained basalt with rare vesicles. Late Tertiary.
MIC	22°77.03N, 98°57.62W	Very fine grained basalt containing no vesicles. Late Tertiary.
BAR	22°95.24N, 97°85.76W	Fine grained basalt. No vesicles. Signs of alteration in some samples. Late Tertiary.
STV	22°94.01N, 97°95.55W	Basalt containing mostly fine grains but with some larger (>2 mm diam.) crystals. Late Tertiary.
ALE	22°93.90N, 97°95.58W	As STV
NTI	22°93.57N, 97°97.55W	As STV
ALD	22°99.19N, 98°05.42W	Very fine grained basalt. No vesicles. Late Tertiary.
ALT	21°02.26N, 98°61.85W	Basalt with many yellow alterations. Fine grained with occasional large elongate vesicles. Late Tertiary.
ARD	20°97.00N, 98°65.81W	Very line grained basalt containing no vesicles. Late Tertiary.
MOL A	20°79.17N, 98°72.32W	Basalt with many white alterations. Mostly fine grained with some larger crystals. Tertiary.
MOL B	(Location as MOL A)	Yellowish coloured igneous rock with large crystals in a finematrix. Very altered. Late Tertiary.
FLO	20°59.13N, 98°62.19W	Light grey flow textured igneous rock with occasional small vesicles. Very fine grain size. Late Tertiary.
HUA	20°55.76N, 98°62.22W	Fine grained basalt containing some small vesicles. Late Tertiary.

Table 1b: Site location with rock type and approximate age for TMVB sites.

TMVB SITES		
Site	**Location**	**General rock type and approx. age.**
MET	20°43.84N, 98°67.45W	Basalt with orange coloured alterations. Fine grain size but with some larger (>1 mm diam.) crystals. Late Tertiary.
ZQU	20°40.98N, 98°68.56W	Fine grained basalt with many small vesicles, and occasional large (>2 mm diam.) ones. Tertiary.
ATO	20°38.69N, 98°72.04W	Fine grained basalt with vesicles of 1–2 mm diam. Late Tertiary.
DYK	20°16.76N, 98°65.06W	Fine grained basalt with vesicles of 1–2 mm diam. Late Tertiary.
FUD	20°15.58N, 98°65.28W	As DYK but more altered appearance. Late Tertiary.
PAC	20°13.36N, 98°70.09W	As FUD.
TEO	19°40.11N, 96°97.45W	Very fine grained basalt containing some small (< l.5 mm diam.) vesicles. Quaternary.
CEL	19°40.08N, 96°97.23W	Fine grained basalt with elongate vesicles. Quaternary.
TUZ	19°38.98N, 96°87.11W	Fine grained basalt with a few larger (approx. l mm diam.) crystals. Some rare vesicles. Quaternary.
ORI	18°94.17N, 97°41.91W	Fine grained basalt with some larger (approx. 1 mm diam.). Abundant small elongate vesicles. Quaternary.
ZAB	18°95.25N, 97°42.02W	Very fine grained basalt containing some very small vesicles. Some pale alterations evident. Quaternary.
PIZ	19°54.06N, 98°12.33W	Fine grained basalt containing many small (<1 mm diam.) vesicles. Slightly weathered. Late Tertiary.
TLA	19°63.54N, 98°l 1.69W	Fines grained basalt containing small vesicles. A few larger elongate vesicles exist in some samples. Late Tertiary.
SAM	19°63.88N, 98°10.79W	Fine grained basalt with some slightly larger crystals. Some small elongate vesicles exist within the basalt. Late Tertiary.
GAS	19°65.69N, 98°09.31W	Fine grained basalt with rare small vesicles. Late Tertiary.
RED	19°77.31N, 98°50.65W	Fine grained basalt matrix surrounding some larger (>lmm diam.) pale crystals. A few very small vesicles. Late Tertiary.
PAN	19°77.03N, 98°50.39W	As RED.
MID	19°77.20N, 98°50.48W	As RED.
MAR	19°78.34N, 98°51.74W	As RED plus some samples have abundant large (>2 mm across) vesicles whilst others have none. Late Tertiary.
POC	19°77.49N, 98°51.68W	As MAR.
SAH	19°77.29N, 98°57.25W	Fine grained basalt with many vesicles between 1 and 5 mm+ across. Late Tertiary.
GUN	19°77.28N, 98°57.34W	As SAH.
BUG	19°83.54N, 98°57.04W	Very fine grained basalt containing no vesicles. Late Tertiary.
TAC	19°83.39N, 98°45.60W	Very fine grained basalt which contains many very small (< l mm diam.) vesicles. Late Tertiary.
RIO	19°80.20N, 98°50.52W	Fine grained basalt with a locally inconsistent distribution of large and smaller vesicles. Obvious white and red coloured alterations. Late Tertiary.

A total of 40 sites were selected within both the TMVB and EAP from which samples were taken of predominantly basaltic late Miocene to Quaternary rocks.

Sampling and laboratory methods

Sampling sites (see Fig. 1) were selected according to rock age, freshness and accessibility of the exposure. A petrol-driven water-cooled rock drill was used to take between six and ten 2.5 cm cores from each site. Each of these were then orientated in situ using a clinometer, magnetic compass and, where possible, a sun compass. The cores were prepared for laboratory analysis using a water-cooled rock saw to cut them into 23 mm long samples.

Various rock magnetic laboratory techniques employed for this study include hysteresis parameters, strong-field thermomagnetic analysis, plus low- and room-temperature susceptibility measurements.

Hysteresis parameters were obtained using a Molspin vibrating sample magnetometer (VSM) with a maximum field of 1 T. The parameters determined were: saturation magnetisation, M_S; saturation remanence, M_{RS}; coercive force, H_C; and the ratio M_{RS}/M_S. A computer controlled horizontal Curie balance was employed to measure strong-field magnetization from room temperature to 700 ^oC in a field of 0.35 T. From the thermomagnetic curve produced, the Curie temperature was estimated using the method of Grommé et al. (1969), and the change in magnetization at 100 ^oC (RM) due to heating was determined. Low temperature susceptibility analyses were carried out by measuring the variation of low-field susceptibility from liquid nitrogen temperature (78 K) to room temperature(293 K). These measurements were done using a computer-controlled Bartington MS2 susceptibility meter with a water-jacketed probe. The relative susceptibility values (RS) were calculated from the temperature versus susceptibility curves. Room temperature susceptibility measurements were carried out using a Bartington MS2 susceptibility meter. A dual frequency Bartington MS2B probe allowed the measurement of low (0.46 kHz) and high (4.6 kHz) frequency susceptibility. Mass susceptibility was calculated for each sample at each frequency. The use of the dual frequency meter also enabled the calculation of frequency dependant susceptibility (χfd%).

Results

Hysteresis parameters

The data gained from the VSM (Table 2) show that the values of M_S are spread between 0.004–2.04 $Am^2 kg^{-1}$, though most of the samples are in the range 0.2–1.21 $Am^2 kg^{-1}$. Such values show there is a significant concentration of magnetic minerals within most of the samples.

Values for the ratio M_{RS}/M_S permit the determination of whether a sample contains multi-domain (MD — M_{RS}/M_S <0.05), single-domain (SD — M_{RS}/M_S ca. 0.5), or a mixture of both types of material ($0.05<M_{RS}/M_S<0.5$) as suggested by O'Reilly (1984). The data gained show a broad range of values between 0.06–0.46 which indicates that the majority of the samples have a mixture of MD and SD grains, though there are samples that are almost completely MD or SD. Coercive force (H_C) values are distributed evenly between 3.38 and 27.64 mT. Some samples exhibit slightly wasp-waisted loops (e.g. SAH 8, Fig. 2) probably due to two different populations of grains, one with hard and one with soft coercivity. The hysteresis loops of other samples such as POZ 7 show magnetic behaviour dominated by paramagnetic material, as identified by stretched loops (see Fig. 2).

Strong-field thermomagnetic behaviour

Samples from each site had their strong-field thermomagnetic behaviour determined and the results are listed in Table 3. The types of thermomagnetic behaviour exhibited by the samples have been classified into different groups. The classifications chosen have been adapted from the methods used by Mankinen et al. (1985) and Sherwood (1988).

Type 1 curves (Fig. 3) show a single ferrimagnetic phase with a low to intermediate (<500 ^oC) Curie temperature. There is a marked difference between heating and cooling curves with an increase in Curie temperature and magnetization in the cooling phase, and therefore the samples have RM values of >1. These type 1 curves are divided into two subgroups: in type1a the Curie temperature on the cooling curve has irreversibly increased to a high temperature phase (>500 ^oC), but there is no disproportionation peak upon heating. Note that RM values for samples of site POZ are

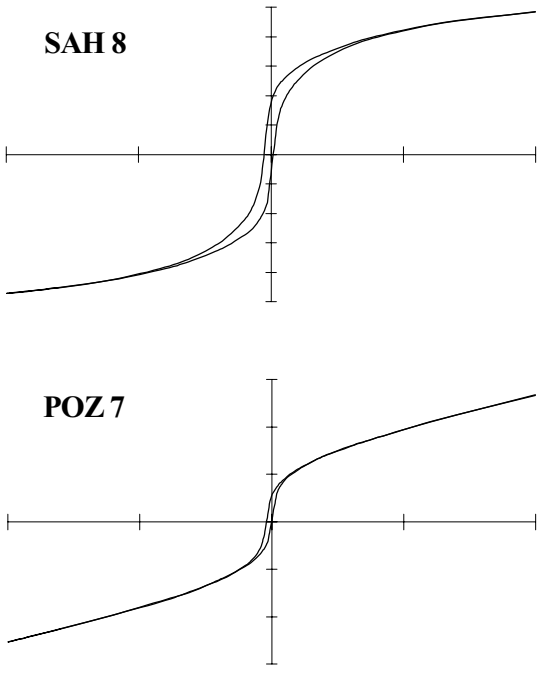

Fig. 2. Hysteresis curves of two samples: SAH 8 shows a wasp waisted loop whilst the curve of POZ 7 is dominated by paramagnetic material.

Table 2: Hysteresis, susceptibility and low temperature susceptibility properties of sites sampled. LFMS — low-field mass susceptibility; HFMS — high-field mass susceptibility; % FDS — percentage frequency dependent susceptibility; RS — relative susceptibility; Ms — saturation magnetization; Mrs — saturation remanent magnetization; Hc — coercive force. Note, all susceptibility figures are site mean values.

Site	LFMS 10^{-8} (m^3kg^{-1})	HFMS 10^{-8} (m^3kg^{-1})	% FDS (χfd%)	RS (χ_{78}/χ_{298})	Ms (Am^2/kg)	Mrs [=SIRM] (Am^2/kg)	Mrs/Ms (Am^2/kg)	Hc (mT)
				EAP SITES				
TEC	1327.12	1312.09	0.50	1.08	1.04	0.29	0.28	27.19
DED	414.34	414.36	-0.01	0.51	0.43	0.06	0.14	8.01
SAN	790.14	781.70	1.07	0.42	0.58	0.09	0.16	6.22
POZ	279.99	283.44	-1.10	0.67	0.11	0.03	0.24	9.69
MIC	2141.99	2138.70	0.16	0.55	2.04	0.41	0.20	17.72
BAR	900.85	902.37	-0.16	0.25	0.76	0.05	0.07	3.90
STV	533.71	537.98	-0.62	0.20	0.46	0.03	0.06	3.38
ALE	764.24	764.81	-0.24	0.52	0.42	0.03	0.07	3.87
NTI	618.11	618.75	-0.16	0.74	0.60	0.08	0.13	14.54
ALD	564.17	564.54	-0.06	0.53	0.50	0.07	0.14	16.17
ALT	382.51	380.30	0.39	1.41	0.40	0.08	0.22	21.80
ARD	1314.16	1304.82	0.85	0.46	0.68	0.11	0.17	5.82
MOL A	415.36	416.54	-0.29	0.95	0.65	0.15	0.23	16.62
MOL B	7.50	7.34	1.85	0.64	0.007	0.0011	0.20	18.10
FLO	130.57	130.52	0.08	0.80	0.26	0.08	0.29	21.95
HUA	93.33	92.72	0.66	1.13	0.20	0.09	0.46	27.64
				TMVB SITES				
MET	104.76	102.23	2.86	1.25	0.09	0.02	0.22	16.50
ZQU	117.31	115.75	1.28	1.45	0.17	0.05	0.27	14.27
ATO	186.55	186.13	0.23	2.41	0.34	0.09	0.26	24.76
DYK	43.46	43.15	0.90	0.63	0.04	0.01	0.26	24.88
FUD	11.97	11.89	0.72	1.05	0.004	0.0008	0.20	10.30
PAC	26.23	25.84	1.75		0.01	0.0027	0.20	17.00
TEO	669.40	669.36	0.00	1.28	0.85	0.07	0.08	5.95
CEL	427.56	426.92	0.15	1.15	0.90	0.15	0.17	12.74
TUZ	292.96	290.89	0.71	1.12	0.50	0.06	0.11	9.07
ORI	606.98	606.43	0.10	1.02	1.20	0.23	0.19	17.30
ZAB	618.93	619.02	0.01	1.14	1.12	0.17	0.15	11.66
PIZ	607.32	602.72	0.96	1.12	0.79	0.20	0.25	20.82
TLA	327.82	327.42	0.12	0.55	0.73	0.18	0.24	18.30
SAM	214.51	212.17	1.20	0.60	0.37	0.12	0.32	13.35
GAS	355.86	355.41	0.11	0.74	0.63	0.09	0.14	9.94
RED	474.94	474.32	0.15	1.19	1.06	0.17	0.16	13.76
PAN	382.04	381.05	0.32	0.50	0.82	0.14	0.17	12.17
MID	559.48	559.57	-0.02	0.58	1.21	0.23	0.19	14.82
MAR	261.50	262.30	-0.28	0.35	0.59	0.12	0.20	7.99
POC	290.60	289.38	0.39	0.44	0.64	0.16	0.25	11.18
SAH	238.10	237.19	0.40	0.47	0.52	0.18	0.34	18.29
GUN	246.70	245.48	0.65	0.73	0.78	0.26	0.33	25.05
BUG	212.63	213.53	-0.42	1.55	0.38	0.08	0.20	17.67
TAC	411.35	410.40	0.25	1.13	0.88	0.11	0.13	14.91
RIO	509.69	508.65	0.22	1.17	1.03	0.12	0.12	11.47

anomalously high and are subsequently labelled type 1a*. Type 1b curves are almost identical to type 1a curves except that a disproportion peak is present on the heating curve. These type 1 curves are interpreted as Ti-rich titanomagnetites which cooled so quickly that no high temperature deuteric oxidation took place, but have since been subjected to low temperature oxidation (maghemitization). The extent of maghemitization is greater in type 1b samples. The fact that these measurements were not performed in a vacuum or a nitrogen atmosphere does make it possible that these samples were oxidized during the experiment. However, it is assumed that this is unlikely due to the small number of samples that exhibit this behaviour.

Type 2 curves (Fig. 4) show a single ferrimagnetic phase with a high Curie temperature, and a decrease in magnetization after heating. This type has been subdivided according to

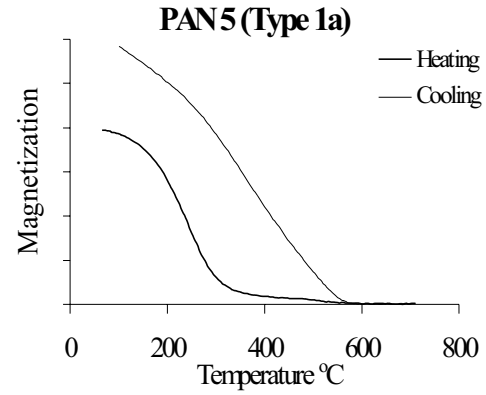

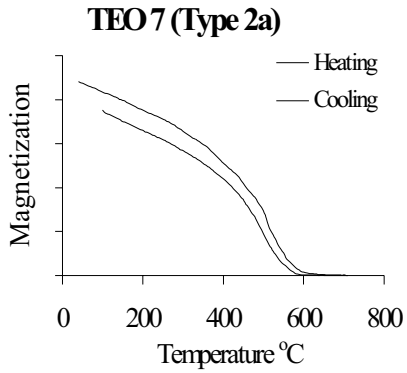

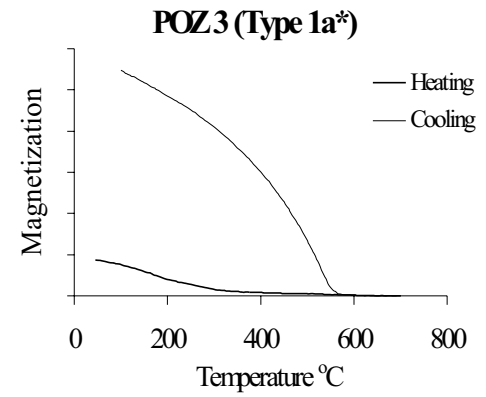

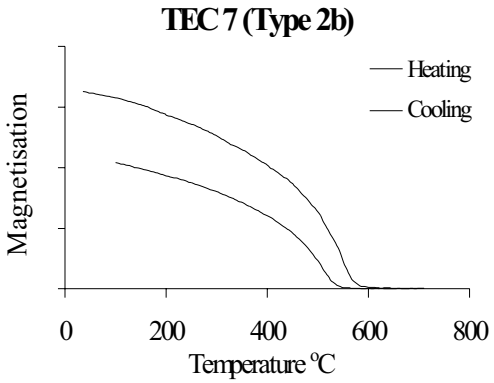

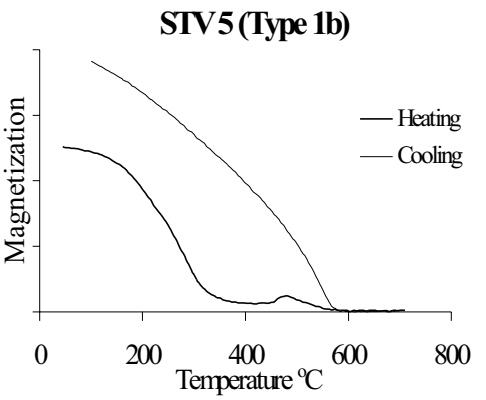

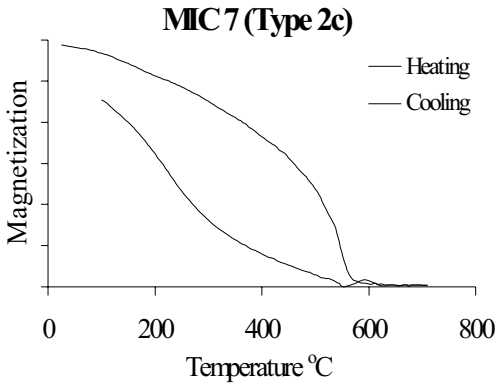

Fig. 3. Examples of all type 1 Curie curves.

Fig. 4. Examples of all type 2 Curie curves.

the degree of irreversibility where type 2c is more irreversible than type 2b which is more irreversible than type 2a. Type 2a curves have similar shaped heating and cooling curves where RM values are between 0.9 and 1 (a <10 % decrease in magnetization upon cooling at 100 °C). The heating and cooling curves of the type 2b plots are similarly shaped but have RM values of <0.9. Type 2c curves also have RM values of <0.9 but exhibit a marked difference in curve shape between heating and cooling. The production of this type 2 magnetic phase is inferred to have been caused by the presence of a Ti-poor titanomagnetite. This Ti-poor phase is unlikely to have been of primary origin as primary titanomagnetites tend to be Ti-rich. Consequently, it is inferred that the Ti-poor phase is caused by the high temperature deuteric oxidation of a Ti-rich titanomagnetite to a Ti-poor titanomagnetite containing ilmenite lamellae.

Type 3 curves (Fig. 5) are similar in most respects to type 2 curves i.e. they exhibit a single ferrimagnetic phase with a high Curie point. The only difference between these and type 2 curves is that the cooling curve crosses the heating curve and therefore the magnetization after cooling is slightly higher than that noted upon heating. Despite this slight difference, the magnetic phase for type 3 curves is assumed to originate by the same process as that of type 2 curves.

Table 3: Strong-field thermomagnetic properties and low temperature susceptibility groupings of selected samples. Tc1 and Tc2 — Curie temperatures; Curie type — classification as described in text; RM — the ratio at 100 °C of magnetization during cooling to magnetization during heating; LTχ Gp. — low temperature susceptibility group.

Samples	Tc 1 (°C)	Tc 2 (°C)	Curie type	RM	LTχ Gp.	Samples	Tc 1 (°C)	Tc 2 (°C)	Curie type	RM	LTχ Gp.
					EAP	SITES					
TEC3	580		2b	0.78	3	**ALE3**	290		1a	1.53	1
TEC7	570		2b	0.66	3	**ALE4**	590		2a	0.90	3/1
DED2	335	540	4b	1.21	1	**NTI2**	600		2b	0.86	3/1
DED6	315	545	4b	1.25	1	**NTI6**	335		1b	1.34	1/3
SAN3	185	500	4b	1.93	1	**ALD7**	485		3	1.09	3/1
SAN5	190	575	4a	1.10	1	**ALD1**	530		2a	1.01	1
POZ3	310		1a*	7.27	4	**ALT5**	200	585	4b	1.21	1
POZ8	315		1a*	5.00	4	**ALT4**	570		2b	0.67	2
MIC1	560		2c	0.84	1	**ARD7**	180		1a	1.79	1
MIC7	560		2c	0.79	1	**ARD2**	320	535	4a	1.02	2
BAR2	310	570	4b	1.26	1	**MOL5**					
BAR9	375		1a	1.76	1	**FLO3**	580		2b	0.68	1
STV5	325		1b	1.56	1	**FLO6**	570		2b	0.65	
STV6	325		1b	1.52	1	**HUA2**	330	595	4b	1.73	
						HUA6	340	575	4b	1.66	
					TMVB	SITES					
MET3	590		2b	0.84		**SAM5**	260		1a	1.89	1
MET6	550		2b	0.86		**SAM2**	210	530	4b	1.22	1
ZQU1	625		2b	0.82		**GAS4**	545		2a	0.94	
ZQU4	580		2a	0.97	2	**GAS6**	570		2a	0.93	1
ATO3	560		2b	0.86	2	**RED3**	530		2a	1.00	3
ATO7	560		2b	0.78	2	**RED8**	580		2b	0.85	3
DYK4	585		2a	0.94		**PAN1**	340	550	1a	1.28	1
DYK8						**PAN5**	305		1a	1.52	1
FUD3						**MID5**	325	550	4b	1.21	1
PAC2						**MID3**	330	560	4a	1.02	1
TEO2	560		2b	0.89	3	**MAR4**	235		1a	1.70	1
TEO7	560		2a	0.90	3	**MAR8**	220		1a	1.75	1
CEL3	540		2a	0.92	2	**POC6**	230		1a	1.83	1
CEL8	540		4a	1.02	2	**POC5**	235		1a	1.72	1
TUZ5	570		2b	0.86	2	**SAH9**	350		1b	1.46	1
TUZ2	560		2b	0.85	2	**SAH4**	350	545	4b	1.26	1
ORI6	560		2a	0.94	2	**GUN5**	590		2b	0.81	3
ORI9	340	545	4a	1.00	3	**GUN1**	535		2a	1.09	1
ZAB2	565		2b	0.86	3	**BUG1**	565		2b	0.81	2
ZAB4	560		2b	0.86	3	**BUG7**	580		2b	0.78	3
PIZ4	575		2a	0.96	3	**TAC2**	590		2b	0.86	3
PIZ2	535		2b	0.86	3	**TAC4**	590		2b	0.88	3
TLA7	275	590	4b	1.13	3/1	**RIO2**	580		2b	0.89	3
TLA4	590		2a	0.97		**RIO5**	590		2b	0.78	3

Type 4 curves (Fig. 5) show two distinct ferrimagnetic phases. One is a low temperature phase and usually occurs at <350 °C. The second phase is higher with Curie temperatures >500 °C. Only the high temperature phase exists on the cooling curve. Most of the type 4 curves also record a higher magnetization after cooling than at the start of heating. The low and high temperature ferrimagnetic phases are interpreted to be caused by Ti-rich and Ti-poor populations of titanomagnetites respectively. The occurrence of the two populations together is inferred to be as a result of partial deuteric oxidation, where some of the Ti-rich titanomagnetite is oxidized to the Ti-poor variety with ilmenite lamellae. As only the high temperature phase is found on the cooling curve this suggests that the low temperature phase is a cation-deficient titanomagnetite, probably as a result of low temperature oxidation (Sherwood 1988).

Of the samples tested on the Curie balance the majority (over 50 %) exhibited type 2 and 3 curves, whilst the sam-

ples with a low Curie temperature make up approximately 22 % of those tested. However, most of the type 4 samples appear to be dominated by the low temperature phase. This indicates that there is approximately an equal number of samples with a primarily Ti-poor phase to those which are dominated by a Ti-rich phase.

Low temperature susceptibility

Information gained from low temperature susceptibility experiments provides some information about the grain size and composition of magnetic minerals. Since this technique was first developed, a generally accepted method of classification and interpretation has evolved (see Radhakrishnamurty et al. 1977; Radhakrishnamurty 1985, 1993; Senanayake & McElhinny 1981; Shaw et al. 1991; Sherwood 1988, 1992; and Sherwood & Basu Mallik 1996), which has been adapted for this study. Classification of a sample is done by observing the shape of the curve gained from the experiment and placing it into one of three main groups: group 1 curves (Fig. 6) exhibit an increase in susceptibility from 78 K to room temperature (293 K) and so have RS values <1. Group 2 curves (Fig. 6) show a decrease in susceptibility from 78 K to 293 K and therefore RS is >1. Group 3 curves (Fig. 6) exhibit a peak at around 125 K whilst the susceptibility values at 78 and 293 K are similar having RS values ca. 1. Samples which exhibit curves with components common to two of the three groups are labelled 3/1 or 1/3 depending on the group from which the dominant component is derived (the first number represents the dominant component group). Unusual samples which show a marked peak at 250 K (group 4) from one site within this study are discussed later.

The mean values of RS (χ_{78}/χ_{293}) for susceptibility groups 1, 2 and 3 are 0.43, 1.54 and 1.14 respectively. These values are similar to those found by Senanayake & McElhinny (1981) and by Sherwood (1988).

Low temperature susceptibility behaviour can not be attributed to any chemical or physical state of magnetic minerals without further information (Radhakrishnamurty 1993), except that the behaviour of group 3 samples is almost certainly caused by MD magnetite. From the information shown in Table 2 it can be seen that the vast majority of samples in group 1 have a Curie temperature indicative of Ti-rich titanomagnetites, and that all the samples that have been classed as group 3 show Curie temperatures which indicate Ti-poor magnetic minerals. These two observations agree with the hypotheses that Ti-rich titanomagnetites will have group 1 behaviour and that MD magnetite will have group 3 behaviour (Radhakrishnamurty 1985, 1993; Senanayake & McElhinny 1981). Like group 3 samples, the samples of group 2 all have Curie temperatures in excess of 480 °C, and this is consistent with the findings of other authors. Unlike group 3 samples however, there are no generally accepted conclusions that can be reached about the behaviour of group 2 samples. Radhakrishnamurty (1977, 1985) ascribes group 2 behaviour to the presence of cation-deficient magnetite, but as in Sherwood (1988), all except one of the samples in this study which have titanomaghemite inversion peaks (Curie type 1b), have group 1

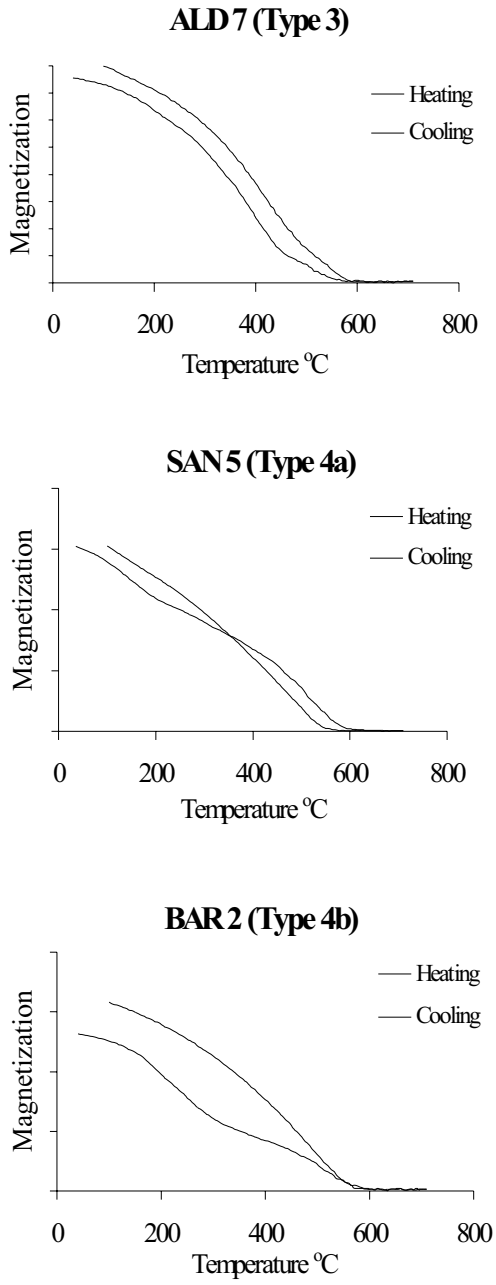

Fig. 5. Examples of Curie curve types 3 and 4.

behaviour. Senanayake & McElhinny (1981) explain group 2 behaviour as a result of the presence of titanomagnetite grains with exsolved ilmenite lamellae. Sherwood & Basu Mallik (1996) suggested that the presence of primary ilmenite is likely to be the principle cause of this type of behaviour. Reflected light microscopy will be able to detect the presence of ilmenite in our samples. The results presented here do not support any definite conclusions concerning this behaviour, although hysteresis plots do suggest the presence of paramagnetic material (possibly ilmenite) in most of the group 2 samples.

Repeatable plots were obtained from the POZ samples (Fig. 6) which have a marked peak at ca. 250 K. Additional-

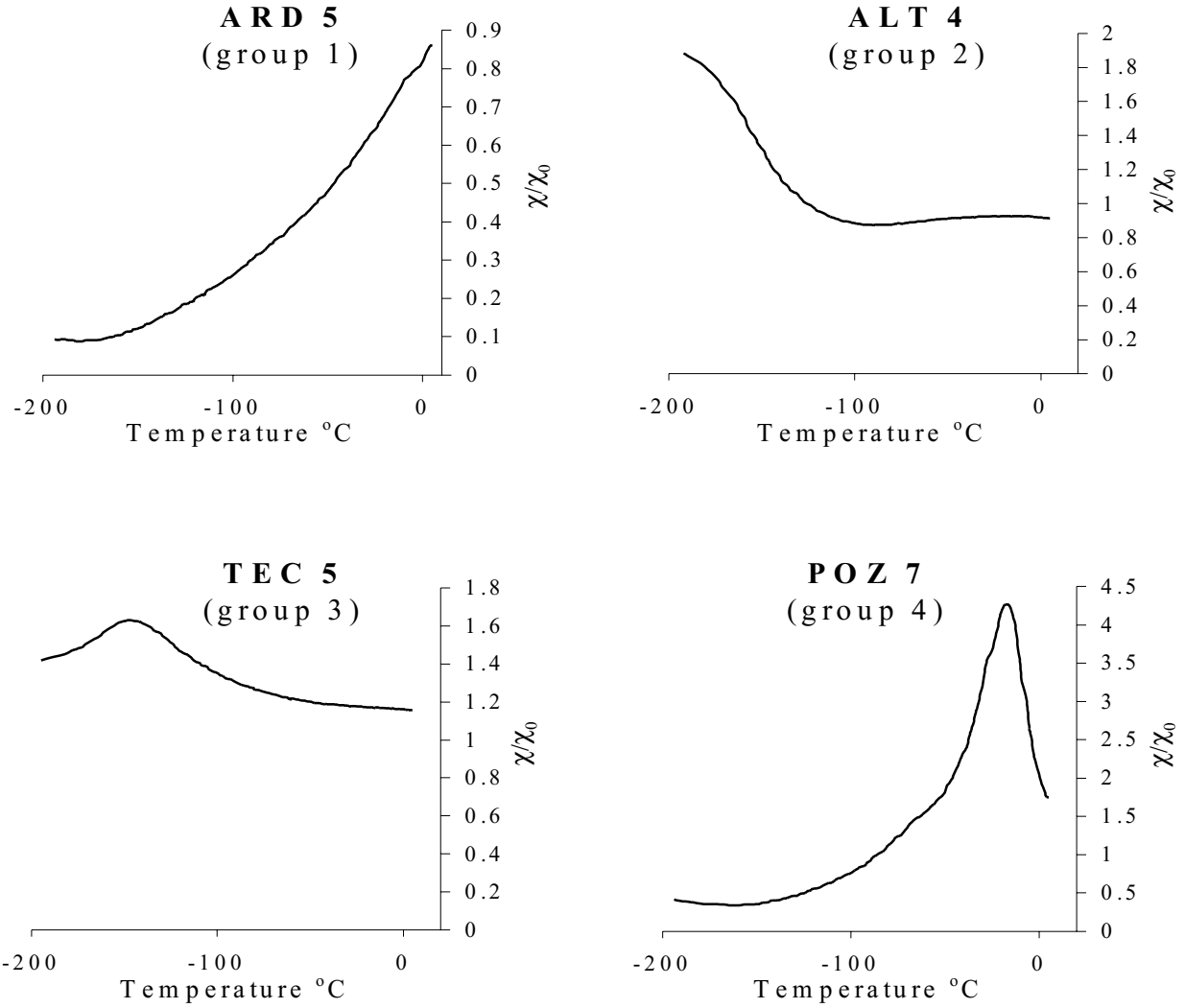

Fig. 6. Typical low temperature susceptibility curves for each group.

ly, thermomagnetic analyses of these samples produced curves with a single low Curie temperature (Ti-rich) phase spread over a range of ca. 100 °C (see Fig. 3). Shaw et al. (1991) and Sherwood (1992) describe similar peaks in their susceptibility analyses, and have attributed them to the unblocking of a low blocking temperature SD titanomagnetite.

Room temperature susceptibility

The values for low- and high-field mass-specific susceptibility (see Table 2) are almost exactly the same for each individual sample site: a scale of the difference between the two values is given by percentage frequency dependent susceptibility (χfd%). From the χfd% value one can tell whether the sample has a significant quantity of ferri- and ferromagnetic grains lying close to the superparamagnetic (SP)/single domain (SD) grain size boundary (Thompson & Oldfield 1986). The values of χfd% obtained for all but 6 of the samples is <1%, i.e. <1% of the overall low frequency susceptibility is contributed to by SP grains. The other samples have χfd% values <3 which is still only a minor overall contribution from SP grains.

Discussion

The rock magnetic data from both the Late Tertiary and Quaternary sites (Table 1) were compared to note any chronological variation in characteristics. The only obvious difference noted is that all the Quaternary samples tested have a high temperature Curie phase, whereas the Tertiary sites have a significant proportion of samples that yielded a low temperature phase. Therefore, all the Quaternary samples have Ti-poor titanomagnetite, whilst the magnetic minerals of the Late Tertiary samples are either Ti-rich or Ti-poor titanomagnetite. There appear to be no other obvious chronological patterns in the remaining rock magnetic data.

A comparison of our data with previous findings from the same region show similar rock magnetic properties (note that results from sites south of latitude 20°N can only be di-

rectly compared as there is no comparable data north of this latitude in the Gulf Coast region). Strong field thermomagnetic analysis by Böhnel (1985, 1997) found samples with Curie temperatures mostly in the range 520 °C to 580 °C which generally agree with the findings of this study. The only slight difference is that this study revealed a greater number of samples dominated by a low temperature Curie phase. Gonzalez et al. (1997) studied the central and western TMVB and show a similar distribution of high and low temperature Curie phases.

Hysteresis parameters obtained by Böhnel (1985) give values for M_{RS}/M_S that are very similar to the values gained in this study, indicating that the vast majority of volcanic rocks from this area have a mixture of SD and MD grains. Only a small minority has either predominantly one or the other domain states.

A comparison between the results of EAP and TMVB samples (Tables 2 and 3) reveal no significant differences in rock magnetic characteristics. Differences do exist however, between samples, and these are assumed to be due to factors such as compositional variation, exposure to weathering etc.

Summary and further work

These results indicate that for the majority of the sites studied there are significant amounts of stable magnetic minerals within the rocks. Therefore, they should be suitable for a paleomagnetic study in which the primary objective will be to obtain site-mean paleomagnetic directions and paleopoles. These values will be used to try to reconstruct the tectonic history of the Gulf Coast region from the Late Tertiary to present day, which is uncertain at this time. A further field season has been completed and these results are being processed at present. The combination of the new data with that presented here will give a more even spatial distribution of site locations. However, these results at least prove that further study is worthwhile.

Acknowledgements: This research was funded by Liverpool John Moores University and Universidad Nacional Autonoma de Mexico. Thanks are due to the staff at the Geomagnetism Laboratory, University of Liverpool where some of the measurements were carried out. We are also grateful to the Gonzalez-Huesca family, Ramon Sandoval and the Instituto de Geofisica for their help with the fieldwork.

References

Barker D.S.,1977: Northern trans-Pecos magmatic province: introduction and comparison with the Kenya Rift. *Geol. Soc. America Bull.*, 88, 1421–1427.

Böhnel H., 1985: Palaeomagnetic investigations of Jurassic to Quaternary rocks from central and southern Mexico (in German). *Ph.D. Thesis*, Univ. Münster, 1–235.

Böhnel H., 1997: Quaternary block rotations in the eastern Trans-Mexican volcanic belt calculated from palaeomagnetic data. In: Delgado, H. (Ed): *Cenozoic volcanism and tectonics of Mexico.Geol. Soc. Amer. Spec. Pap.,* in press.

Burbach G. V., Frohlich C., Pennington W.D. & Matsumoto T., 1984: Seismicity and tectonics of the subducted Cocos plate. *Journal of Geophysical Research,* 89, 7719–7735.

Cantagrel J.M. & Robin C., 1979: K-Ar dating on eastern Mexican volcanic rocks relations between the andesitic and alkaline provinces. *Journal of Volcanology and Geothermal Research,* 5, 99–114.

Gonzalez S., Sherwood G., Böhnel H. & Schnepp E., 1997: Palaeosecular variation in central Mexico over the last 30,000 years: the record from lavas. *Geophysical Journal International*, 130, 201–219.

Grommé S., Wright T.L. & Peck D.L., 1969: Magnetic properties and oxidation of iron-titanium oxide minerals in Alae and Makaopuhi lava lakes, Hawaii. *Journal of Geophysical Research,* 74, 5277–5293.

Mankinen E.A., Prevot M. & Gromme C.S., 1985: The Steens Mountain (Oregon) geomagnetic polarity transition 1: directional history, duration of episodes, and rock magnetism. *Journal of Geophysical Research, 90,* 10393–10416.

Nixon G.T., 1982: The relationship between Quaternary volcanism in central Mexico and the seismicity and structure of subducted oceanic lithosphere. *Geol. Soc. Amer. Bull.*, 93, 514–523.

Nixon G.T., Demant A., Armstrong R.L. & Harakal J.E., 1987: K-Ar and geologic data bearing on the age and evolution of the TMVB. *Geofisica Internacional,* 26, 109–158.

O'Reilly W., 1984: Rock and mineral magnetism. *Blackie*, Glasgow, 1–220.

Parker D.F. & McDowell F.W., 1973: K-Ar geochronology and eruptive history of Oligocene volcanic rocks, Davies Mountains, trans-Pecos, Texas. *Geological Society of America, Abstracts with programs*, 5, 764–765.

Radhakrishnamurty C., 1985: Identification of titanomagnetites by simple magnetic techniques and application to basalt studies. *Journal of the Geological Society of India,* 26, 640–651.

Radhakrishnamurty C., 1993: Magnetism and basalts. *Memoir of the Geological Society of India,* 26, 1–209.

Radhakrishnamurty C., Likhite S.D. & Sahasrabudhe, P.W., 1977: Nature of magnetic grains and their effect on the remanent magnetization of basalts. *Physics of the Earth and Planetary Interiors,* 13, 289–300.

Robin C., 1976: Simultaneous presence of magmatism of opposite tectonic significance in eastern Mexico. *Bull. Soc. Géol. France,* 18, 1637–1645 (in French).

Robin C., 1982: Mexico. In: Thorpe R.S. (Ed): *Andesites, orogenic andesites, and related rocks. Wiley,* New York, 137–147.

Robin C. & Tournon J., 1978: Spatial relations of andesitic and alkaline provinces in Mexico and Central America. *Canad. J. Earth Sci.,* 15, 1633–1641.

Senanayake W.E. & McElhinny M.W., 1981: Hysteresis and susceptibility characteristics of magnetite and titanomagnetites: interpretation of results from basaltic rocks. *Physics of the Earth and Planetary Interiors,* 26, 47–55.

Shaw J., Sherwood G.J., Musset A.E., Rolph T.C., Subbarao K.V. & Sharma P.V., 1991: The strength of the geomagnetic field at the Cretaceous-Tertiary boundary palaeointensity results from the Deccan Traps (India) and the Disko Lavas (Greenland). *Journal of Geomagnetism and Geoelectricity,* 43, 395–408.

Sherwood G.J., 1988: Rock magnetic studies of Miocene volcanics in eastern Otago and Banks Peninsula, New Zealand: comparison between Curie temperature and low temperature susceptibility behaviour. *New Zealand Journal of Geology and Geophysics,* 31, 225–235.

Sherwood G.J., 1992: Some rock magnetic properties of mid-Cretaceous basalts from Israel and India (Rajmahal Traps), and their bearing on palaeointesity experiments. *Physics of the Earth and Planetary Interiors,* 70, 237–242.

Sherwood G.J. & Basu Mallik S., 1996: A palaeomagnetic and rock magnetic study of the northern Rajmahal Volcanics, Bihar, India. *Journal of Southeast Asian Earth Sciences,* 13, 123–131

Thompson R. & Oldfield F., 1986: Environmental magnetism. *Allen and Unwin*, London, 1–227.

Thorpe R.S., 1977: Tectonic significance of alkaline volcanism in eastem Mexico. *Tectonophysics,* 40, 19–26.